

## NUMERICAL APPROACH TO INVISCID SEPARATED FLOWS WITH INFINITELY-LONG CUSP-ENDED STAGNATION ZONE

C. I. Christov and M. D. Todorov

### 1. Introduction

The separated flows attracted the attention as early as in the Seventies of the previous century. Helmholtz [9] posed the problem as matching between a potential flow and a stagnant zone at priori unknown free boundaries which are tangential discontinuities and where the balance of normal stresses (the pressure) holds. Krichhoff [12] came up with the first solution for the ideal jet flowing out from a hole when the detachment points were known in advance. For blunt bodies an additional condition for smooth separation (called now Brillouin-Villat condition [1, 15]) is to be satisfied. The first approximate solution for a blunt body (the circular cylinder) was provided by Brodetsky [2] who came up with a parabolic expanding at infinity shape of the stagnation zone. To a reasonable degree this solution was qualitatively confirmed by the Navier-Stokes calculations [11, 7, 8].

Another Helmholtz flow radically different from the Brodetsky flow takes place when the breadth of the stagnation zone decreases at infinity forming an infinite cusp. Glimpses of this kind of flow were first encountered in the direct difference solutions [10, 13] but due to the limitation of computers the shape of the zone was not conclusive and later on the model was virtually abandoned in the literature. We also found this cusp-ended stagnation zones [3, 4, 5] by means of difference scheme and confirmed by integral-method calculations [14].

The gist of our approach is to make use of two different coordinate systems: the ubiquitous polar coordinate system (turning out to be ineffective for the case of infinite stagnation zones extending far away from the rear end of body) and the parabolic coordinate system the latter being topologically more suited for solving Laplace equation outside infinitely long stagnation zones. We initiate the calculations in polar coordinates switching to parabolic coordinates after the stagnation zone has fairly well developed and has become long enough.

In our previous works we solved the equation for shape function in parabolic coordinates. Although this algorithm turned out to work well for Brodetsky flow, it was not very convenient for cusp-ended stagnation zones leading to hard to tackle numerical instabilities.

Here we use the parabolic coordinates for Laplace equation only and treat the shape function exclusively in terms of the polar coordinates where the governing equation is stable. At each global iteration the solution for stream function is returned from parabolic to cylindrical coordinates and then used in the equation for the shape function.

## 2. Posing the problem

Consider the steady inviscid flow past a circle – the cross section of an infinitely long circular cylinder. The direction of the flow coincides with the line  $\theta = 0, \pi$  of the polar coordinates and the leading stagnation point of the flow is situated in the point  $\theta = \pi$ . For the sake of convenience we recall here the connection between parabolic and Cartesian coordinates

$$x = \frac{1}{2}(\tau^2 - \sigma^2), \quad \sigma \geq 0; \quad y = \sigma\tau, \quad -\infty > \tau > \infty.$$

Dimensionless variables are introduced as follows

$$\psi' = \frac{\psi}{LU_\infty}, \quad r' = \frac{r}{L}, \quad q = \frac{p - p_c}{\frac{1}{2}\rho U_\infty^2}, \quad \sigma = \sqrt{L}\sigma', \quad \tau = \sqrt{L}\tau', \quad \kappa = \frac{p_\infty - p_c}{\frac{1}{2}\rho U_\infty^2}, \quad (2.1)$$

where  $L$  is the characteristic length of the body ( $2a$  for a cylinder of radius  $a$ ),  $U_\infty$  – velocity of the undisturbed flow;  $p_c$  – the pressure inside the stagnation zone;  $p_\infty$  – the pressure at infinity. Without fear of confusion the primes will be omitted henceforth.

The parameter  $\kappa$  is called cavitation number. For flows with stagnation zones it is trivially equal to zero since the pressure must be continuous at infinity and hence  $p_c = p_\infty$ . For cavitation problems  $\kappa$  can assume nontrivial values since  $p_c$  is not forced to be equal to  $p_\infty$ . Let us mention in passing that in general the pressure in the stagnation zone can also be a function of the longitudinal variable accounting thus for the interaction with the boundary layer.

### 2.1. Coordinate systems

In terms of the two coordinate systems (cylindrical and parabolic) Laplace equation for the stream function function  $\psi$  reads:

$$\psi_{rr} + \frac{1}{r}\psi_r + \frac{1}{r^2}\psi_{\theta\theta} = 0, \quad \text{or} \quad \frac{1}{\sigma^2 + \tau^2}(\psi_{\sigma\sigma} + \psi_{\tau\tau}) = 0. \quad (2.2)$$

The undisturbed uniform flow at infinity is given by

$$\psi|_{r \rightarrow \infty} \approx rU_\infty \sin \theta, \quad \text{or} \quad \psi|_{\sigma \rightarrow \infty, \tau \rightarrow \pm \infty} \approx \sigma\tau U_\infty. \quad (2.3)$$

On the combined surface “body+stagnation zone” hold two conditions. The first condition secures that the said boundary is a stream line (say of number “zero”)

$$\psi(R(\theta), \theta) = 0, \quad \theta \in [0, 2\pi] \quad \text{or} \quad \psi(S(\tau), \tau) = 0, \quad \tau \in [-\infty, \infty], \quad (2.4)$$

where  $R(\theta)$ ,  $S(\tau)$  are the shape functions of the total boundary in polar or parabolic coordinates, respectively. Here and henceforth we use the notation  $\Gamma_1$  for the portion of boundary representing the rigid body (the cylinder) and  $\Gamma_2$  – for the free streamline.

Let  $\theta^*$  and  $\tau^*$  be the magnitudes of the independent coordinates for which the detachment of flow occurs. As far as we consider only the case when the stagnation zone is situated behind the body then the portion of  $\Gamma_2$  which describes the free line for the “upper part” of the flow is defined as  $0 \leq \theta \leq \theta_u^*$  or  $\tau \geq \tau_u^*$ , respectively. The “lower part” is described by the inequalities  $\theta_l^* \leq \theta \leq 2\pi$  and  $\tau \leq -\tau_l^*$ . On  $\Gamma_2$  the shape function  $R(\theta)$  is unknown and it is to be implicitly identified from Bernoulli integral with the pressure equal to a constant (say,  $p_c$ ) which is the second condition holding on the free boundary. For the two coordinate systems one gets the following equations for shape functions  $R(\theta)$  or  $S(\tau)$ :

$$\left[ q + \frac{\psi_\theta^2}{r^2} + \psi_r^2 \right]_{r=R(\theta)} = 1, \quad \text{or} \quad \left[ q + \frac{(\psi_\sigma^2 + \psi_\tau^2)}{\sigma^2 + \tau^2} \right]_{\sigma=S(\tau)} = 1, \quad (2.5)$$

$$0 \leq \theta \leq \theta_u^*, \quad \tau_u^* < \tau < \infty.$$

For symmetric bodies it is sufficient to solve the boundary value problem (2.2), (2.3), (2.4), (2.5) in one of the halves of the flow (say, the upper half) and additional conditions are added

$$\frac{\partial \psi}{\partial \theta} = 0, \quad \theta = 0, \pi \quad \text{or} \quad \frac{\partial \psi}{\partial \tau} = 0, \quad \tau = 0. \quad (2.6)$$

In the general case of non-symmetric bodies the problem must be solved in the entire plane which implies that (2.5) must be imposed also on the other free line (the line which lies in the lower semi-plane), if it exists.

## 2.2. Scaled Variables

The outlined boundary value problem is very inconvenient for numerical treatment mainly because of two reasons. The first is that the boundary lines are not coordinate lines. The second is that the shape function of the stagnation zone must be implicitly identified from the additional boundary condition (2.5). A way to overcome these difficulties is to scale the independent variable ( $\theta$  or  $\tau$ ) by the shape function  $R(\theta)$  or  $S(\tau)$ , respectively. Such a manipulation renders the original physical domain under consideration into a region with fixed boundaries, the latter being coordinate lines. In addition the Bernoulli integral becomes an explicit equation for the shape function of the free boundary. Scaling the independent variable proved very efficient in numerical treatment of inviscid or viscous flows with free boundaries (see, e.g., [6]).

We define after [3, 4, 5] new independent coordinates:

$$\eta = rR^{-1}(\theta), \quad \eta = \sigma - S(\tau)$$

in place of the polar radius  $r$  or the parabolic coordinate  $\sigma$ , respectively.

In the virtue of these transformations of boundary  $\Gamma = \Gamma_1 + \Gamma_2$  the region becomes a semi-infinite strip in both coordinate systems

$$[1 \leq \eta < \infty, 0 \leq \theta \leq \pi] \quad \text{or} \quad [0 \leq \eta < \infty, 0 < \tau < \infty].$$

We treat the two coordinate systems in a uniform way denoting  $\xi \equiv \theta$  or  $\xi \equiv \tau$  depending on the particular case under consideration. In terms of the new coordinates  $(\eta, \xi)$ ,

the stream function is a compound function  $\tilde{\psi}(\eta, \theta) \equiv \psi(r(\eta, \xi), \xi)$  or  $\tilde{\psi}(\eta, \tau) \equiv \psi(\sigma(\eta, \xi), \xi)$  but in what follows we drop the “tilde” without fear of confusion. The Laplace equation takes then the form

$$a\psi_{\eta\eta} - 2b\psi_{\eta\xi} + \psi_{\xi\xi} + d\psi_{\eta} = 0 \quad (2.7)$$

where

$$a \equiv \eta^2 \left[ 1 + \left( \frac{R'}{R} \right)^2 \right], \quad b \equiv \eta \frac{R'}{R}, \quad d \equiv \eta \left[ 1 - \frac{R''}{R} + 2 \left( \frac{R'}{R} \right)^2 \right];$$

or

$$a \equiv 1 + S'^2, \quad b \equiv S', \quad d = -S''.$$

In fact the “relative” function  $\bar{\psi}$  is used

$$\bar{\psi}(\eta, \theta) = \psi(\eta, \theta) - \eta R(\theta) \sin \theta, \quad \bar{\psi}(\eta, \tau) = \psi(\eta, \tau) - [\eta + S(\tau)]\tau,$$

which is obviously a solution to eq.(2.7) and which we loosely call stream function. The asymptotic boundary condition then becomes

$$\bar{\psi} \Big|_{\eta=\eta_\infty} = 0 \quad \text{or} \quad \bar{\psi} \Big|_{\eta=\eta_\infty, \tau=\pm\tau_\infty} = 0, \quad (2.8)$$

while the non-flux condition on  $\Gamma$  transforms as follows

$$\bar{\psi} \Big|_{\eta=1} = -\eta R(\theta) \sin \theta \quad \text{or} \quad \bar{\psi} \Big|_{\eta=0} = -S(\tau)\tau. \quad (2.9)$$

Thus eqs.(2.7), (2.8), (2.9) define a well posed boundary value problem provided that functions  $R(\theta)$  and  $S(\tau)$  are known. On the other hand in the portion  $\Gamma_2$  of the boundary (where these functions are unknown) they can be evaluated from the Bernoulli integral (2.5) which now becomes an equation for the shape function

$$\frac{R^2 + R'^2}{R^4} \left[ \frac{\partial \bar{\psi}}{\partial \eta} \Big|_{\eta=1} + R(\theta) \sin \theta \right]^2 = 1, \quad \text{or} \quad \frac{1 + S'^2}{S^2 + \tau^2} \left[ \frac{\partial \bar{\psi}}{\partial \eta} \Big|_{\eta=0} + \tau \right]^2 = 1, \quad (2.10)$$

$$0 \leq \theta \leq \theta_u^*, \quad \tau_u^* \leq \tau < \infty.$$

### 3. Forces Exerted on the body

The presence of a stagnation zone breaks the symmetry of the integral for the normal stresses and hence D'Alembert paradox ceases to exist, i.e. the force exerted from the flow upon the body is no more equal to zero. Denote by the outward normal vector to the contour  $\Gamma$ . Then the force acting upon the contour is given by

$$= - \oint_{\Sigma} p ds = - \oint_{\Sigma} (q + p_c) ds \stackrel{\text{def}}{=} \rho a U_\infty^2 [C_x + C_y], \quad (3.1)$$

where  $C_x$  and  $C_y$  are the dimensionless drag coefficient and the lifting force. Note that the boundary  $\Gamma$  (rigid or free) is defined by the equation  $\zeta - F(\xi) = 0$ , where  $\zeta \equiv r$ ,  $F(\xi) \equiv R(\theta)$  or  $\zeta \equiv \sigma$ ,  $F(\xi) \equiv S(\tau)$ . The unit vector normal to the line  $\Gamma$  and the elementary length along  $\Gamma$  are expressed as

$$= \left( \frac{\xi}{\sqrt{g_{11}}} - \frac{F'(\xi)\zeta}{\sqrt{g_{22}}} \right) \left[ \frac{1}{g_{11}} + \frac{F'^2(\xi)}{g_{22}} \right]^{-\frac{1}{2}}, \quad ds = d\xi \sqrt{g_{11}F'^2(\xi) + g_{22}}, \quad (3.2)$$

where  $g_{11} = 1, g_{22} = R(\theta), \quad \text{or} \quad g_{11} = \sqrt{S^2 + \tau^2}, g_{22} = \sqrt{S^2 + \tau^2}.$  (3.3)

are the components of the metric tensor in the two coordinate systems. Respectively  $\zeta = r$ ,  $\xi = \theta$  or  $\zeta = \sigma$ ,  $\xi = \tau$  are the unit vectors tangential to the coordinate lines. These are connected to the Cartesian basis vectors and as follows

$$\xi = \frac{1}{\sqrt{g_{22}}} \left( \frac{\partial x}{\partial \xi} + \frac{\partial y}{\partial \xi} \right) \quad \text{and} \quad \zeta = \frac{1}{\sqrt{g_{11}}} \left( \frac{\partial x}{\partial \zeta} + \frac{\partial y}{\partial \zeta} \right),$$

where  $x$  and  $y$  are the Cartesian coordinates. Upon substituting the above relations into (3.1) and after obvious manipulations we obtain for the drag and lifting-force coefficients the following expression

$$\begin{aligned} C_x &= 2 \int_{\theta_u^*}^{\pi} q [R(\theta) \cos \theta + R'(\theta) \sin \theta] d\theta & C_x &= 2 \int_0^{\tau_u^*} q [S(\tau) + S'(\tau)\tau] d\tau \\ & \text{or} & & \\ C_y &= 2 \int_{\theta_u^*}^{\pi} q [R(\theta) \sin \theta - R'(\theta) \cos \theta] d\theta & C_y &= 2 \int_0^{\tau_u^*} q [\tau - S'(\tau)S] d\tau. \end{aligned} \quad (3.4)$$

where the dimensionless pressure is given by

$$q = 1 - \frac{R^2 + R'^2}{R^4} \left[ \left. \frac{\partial \bar{\psi}}{\partial \eta} \right|_{\eta=1} + R(\theta) \sin \theta \right]^2 \quad \text{or} \quad q = 1 - \frac{1 + S'^2}{S^2 + \tau^2} \left[ \left. \frac{\partial \bar{\psi}}{\partial \eta} \right|_{\eta=0} + \tau \right]^2. \quad (3.5)$$

## 4. Difference Scheme and Algorithm

### 4.1. A Splitting scheme for Laplace equation

By means of the scaled coordinates the physical region under consideration has been transformed into a computational domain with fixed boundaries. This radically simplifies the implementation of the difference scheme enabling one to use the economic schemes of coordinate splitting. The only numerical difficulty that remains is connected with the fact that the domain is infinite. For the purposes of the numerical solution, the domain must be reduced to finite one after appropriately choosing the ‘‘actual infinities’’. In the case of polar coordinates the domain is infinite with respect to coordinate  $\eta$  only and it fully suffices to select sufficiently large number  $\eta_\infty$  and to consider the rectangle:  $[0 \leq \theta \leq \pi; 1 \leq \eta \leq \eta_\infty]$ . In the case of parabolic coordinates an actual infinity is to be specified also for the  $\tau$ -coordinate, namely  $\tau_\infty$  and to consider the rectangle:  $[0 \leq \tau \leq \tau_\infty; 0 \leq \eta \leq \eta_\infty]$ .

In both directions we employ non-uniform mesh. The first and the last  $\eta$ -lines are displaced (staggered) from the respective domain boundaries on a half of the adjacent value of the spacing. Thus on two-point stencils second-order approximation for the boundary conditions is achieved. The non-uniformity of the mesh enables us to improve the accuracy near the body and to reduce the number of points at infinity.

In  $\theta$ -direction the mesh is not staggered but it is once again non-uniform being very dense in the vicinity of the rear stagnation point, i.e. in the vicinity of  $\theta = 0$  which is of crucial importance when acknowledging the infinity in cylindrical coordinates. It is desirable to have the ‘‘actual infinity’’ in cylindrical coordinates as larger as possible in order to prepare the ground for switching to the parabolic coordinates.

The formulas for the staggered non-uniform  $\eta$ -mesh and for the non-uniform  $\theta$ -meshe can be found in our previous contributions [3, 4]. Note that  $M$  is the number of points in  $\theta$ - or  $\tau$ -direction in the upper half plane of the flow. Respectively  $M$  is the total number of grid lines in  $\eta$ -direction.

The connection between the  $\tau$ -mesh and  $\theta$ -mesh is derived on the basis of the connections between the two coordinate systems, namely

$$\tau_j = \sqrt{R(\theta_j) \cos \theta_j + R(\theta_j)}, \quad \text{if } 0 \leq \theta_j \leq \pi; \quad S_j = \sqrt{2R_j - \tau_j^2}, \quad (4.1)$$

and these relations can be transformed when necessary to calculate  $S_j, \tau_j$  from  $R_j, \theta_j$  or vice versa.

Let us now denote the spacings of the mesh by  $h_{i+1} \equiv \eta_{i+1} - \eta_i$ ,  $i = 1, \dots, M$  and  $g_{j+1} \equiv \xi_{j+1} - \xi_j$ ,  $j = 1, \dots, N-1$ . The choices for the mesh points and for  $\eta_\infty$  are of crucial importance for the successful solution of the problem. Then the coefficients and operators in (2.7) are approximated as follows:

$$a_{ij} = \eta_i^2 \left[ 1 + \left( \frac{\Lambda_2 R_j}{R_j} \right)^2 \right], \quad b_{ij} = \eta_{ij} \frac{\Lambda_2 R_j}{R_j}, \quad d_{ij} = \eta_i \left[ 1 - \frac{\Lambda_{22} R_j}{R_j} + 2 \left( \frac{\Lambda_2 R_j}{R_j} \right)^2 \right],$$

$$a_{ij} = 1 + (\Lambda_2 S_j)^2, \quad b_{ij} = \Lambda_2 S_j, \quad d_{ij} = -\Lambda_{22} S_j,$$

where

$$\Lambda_1 \phi_{ij} \equiv \frac{h_i^2 \phi_{i+1,j} + (h_{i+1}^2 - h_i^2) \phi_{ij} - h_{i+1}^2 \phi_{i-1,j}}{h_i h_{i+1} (h_i + h_{i+1})} = \frac{\partial \phi}{\partial \eta} \Big|_{ij} + O(h_i h_{i+1}),$$

$$\Lambda_2 \phi_{ij} \equiv \frac{g_j^2 \phi_{i,j+1} + (g_{j+1}^2 - g_j^2) \phi_{ij} - g_{j+1}^2 \phi_{i,j-1}}{g_j g_{j+1} (g_j + g_{j+1})} = \frac{\partial \phi}{\partial \xi} \Big|_{ij} + O(g_j g_{j+1}),$$

$$\Lambda_{11} \phi_{ij} \equiv 2 \frac{h_i \phi_{i+1,j} - (h_i + h_{i+1}) \phi_{ij} + h_{i+1} \phi_{i-1,j}}{h_i h_{i+1} (h_i + h_{i+1})} = \frac{\partial^2 \phi}{\partial \eta^2} \Big|_{ij} + O(h_i h_{i+1}),$$

$$\Lambda_{22} \phi_{ij} \equiv 2 \frac{g_i \phi_{i,j+1} - (g_j + g_{j+1}) \phi_{ij} + g_{j+1} \phi_{i,j-1}}{g_i g_{j+1} (g_j + g_{j+1})} = \frac{\partial^2 \phi}{\partial \xi^2} \Big|_{ij} + O(g_j g_{j+1}),$$

$$\Lambda_{12} \phi_{ij} \equiv \Lambda_1 \Lambda_2 \phi_{i,j+1} = \frac{\partial^2 \phi}{\partial \eta \partial \xi} \Big|_{ij} + O(h_i h_{i+1} + g_j g_{j+1}),$$

for  $i = 2, \dots, M-1, \quad j = \dots, N$

For second order of approximation the pointwise variation of the nonuniform mesh must be smooth enough, in the sense that  $h_i \approx O(h_{i+1})$ ,  $g_j \approx O(g_{j+1})$ .

The symmetry conditions  $\psi_{i,0} = \psi_{i,2}$  and  $\psi_{i,N+1} = \psi_{i,N-1}$  couple the above system. The implementation of the conditions at infinity and for non-flux through  $\Gamma$  is straightforward. The dynamic condition is treated in the next subsection.

We solve the boundary value problem iteratively by means of splitting method. Upon introducing fictitious time we render the equation to parabolic type and then employ the so-called scheme of stabilising correction [16]. It is at no deviation from our above cited previous works and we shall not dwell on it here.

To calculate afterwards the forces acting upon the body we use the simple formulas for numerical integration based on the trapezoidal rule, which are consistent with the overall second-order approximation of the scheme.

#### 4.2. Difference Approximation for the Free Boundary

The equations (2.10) can be resolved for the derivatives  $R'(\theta)$  or  $S'(\tau)$  when the following conditions are satisfied:

$$\begin{aligned} Q(\theta) &\stackrel{\text{def}}{=} \frac{R^2(\theta)}{T^2} > 1, \quad T = \left. \frac{\partial \bar{\psi}}{\partial \eta} \right|_{\eta=1} + R(\theta) \sin \theta \\ \text{or} \\ Q(\tau) &\stackrel{\text{def}}{=} \frac{S^2(\tau) + \tau^2}{T^2} > 1, \quad T = \left. \frac{\partial \bar{\psi}}{\partial \eta} \right|_{\eta=0} + \tau \end{aligned} \quad (4.2)$$

The above inequalities are trivially satisfied in the vicinity of the leading-end stagnation point inasmuch as that for  $\theta \rightarrow \pi$  (or  $\tau \rightarrow 0$ ) one has  $T \rightarrow 0$  and hence  $\frac{R^2}{T^2} \rightarrow \infty$  or  $\frac{S^2 + \tau^2}{T^2} \rightarrow \infty$ . In the present work we use the dynamic condition (2.5) in polar coordinates only, so that we present here just the relevant scheme in polar coordinates without going into the details for parabolic coordinates.

Suppose that the set functions  $\psi_{ij}^\alpha, R_j^\alpha, S_j^\alpha, T_j^\alpha$  are known from the previous global iteration, say of number  $\alpha$ .<sup>1</sup> We check the satisfaction of (4.2) beginning from the point  $\theta = 0$  (or  $\tau = \tau_\infty$ ) and continue with increasing  $\theta$  (decreasing  $\tau$ ). Let  $j_u^* + 1$  be the last point where (4.2) is satisfied and, respectively  $j_u^* -$  the first one where it is not (polar coordinates). In the same manner are conducted the calculations in the “lower” half of the plane when necessary. The position  $\theta_u^*$  of the detachment point is captured by means of a linear interpolation

$$\theta_u^* = \frac{\theta_{j_u^*+1} Q_{j_u^*} - \theta_{j_u^*} Q_{j_u^*+1}}{Q_{j_u^*} - Q_{j_u^*+1}} \quad \rightarrow \quad g_u^* = \theta_u^* - \theta_{j_u^*+1} .$$

For the shape function  $\hat{R}_j$  of free line is solved the following difference scheme

$$\hat{R}_{j-1} - \hat{R}_j = g_j \frac{\hat{R}_j + \hat{R}_{j-1}}{2} \sqrt{\frac{1}{2} \left[ \left( \frac{R_j^\alpha}{T_j^\alpha} \right)^2 + \left( \frac{R_{j-1}^\alpha}{T_{j-1}^\alpha} \right)^2 \right]} - 1 \quad \text{for } j = j_u^*, \dots, 1, \quad (4.3)$$

whose approximation is  $O(g_j^2)$ . Only in the in the detachment point the difference scheme is different, specifying in fact the initial (“inlet”) condition, namely

$$\hat{R}_{j_u^*} - R(\theta_u^*) = g_u^* \frac{R(\theta_u^*) + \hat{R}_{j_u^*}}{2} \sqrt{\frac{1}{2} \left[ \frac{R_{j_u^*}^\alpha}{T_{j_u^*}^\alpha} \right]^2} - 1 \quad (4.4)$$

where  $R$  without a superscript or “hat” stands for the known boundary of rigid body.

In the end a relaxation is used for the shape-function of the free boundary at each global iteration according to the formula:

$$R^{\alpha+1} = \omega \hat{R}_j + (1 - \omega) R_j^\alpha$$

where  $\omega$  is called relaxation parameter.

<sup>1</sup>We distinguish here between global and local iteration, the latter referring to the time-stepping of the coordinate splitting method.

### 4.3. The general Consequence of the Algorithm

Each global iteration contains two stages. On the first stage, the difference problem for Laplace equation is solved iteratively either in polar or in parabolic coordinates (depending on the development of the stagnation zone). The internal iterations (time steps with respect to the fictitious time in the splitting procedure) are conducted until convergence is achieved in the sense that the uniform norm is lesser than  $\approx \varepsilon_2 = 10^{-6}$ . Thus the new iteration for stream function  $\psi_{ij}^{\alpha+1}$  is obtained.

The polar coordinates appear to be instrumental only on the first several (7-10) global iterations. When the rearmost cusp point of the stagnation zone reaches 10 diameters of cylinder (calibres), the current-iteration values of the sought functions are transformed to parabolic coordinates and thence the calculations for the stream function continue solely in terms of parabolic coordinates.

The second stage of a global iteration consists in solving the difference problem for the free surface in polar coordinates. The transition to and from parabolic coordinates is done according to (4.1). Note that there is one-to-one correspondence between the points in polar and parabolic coordinates and hence between the respective values of the scalar set functions  $\psi$  and  $R$ .

The criterion for convergence of the global iterations is defined by the convergence of the shape function as being the most sensitive part of the algorithm, namely the global iterations are terminated when  $\max_j \left| (R_j^{\alpha+1} - R_j^\alpha) / R_j^{\alpha+1} \right| < 10^{-4}$ . Then the velocity, pressure, and the forces exerted from the flow upon the body are calculated.

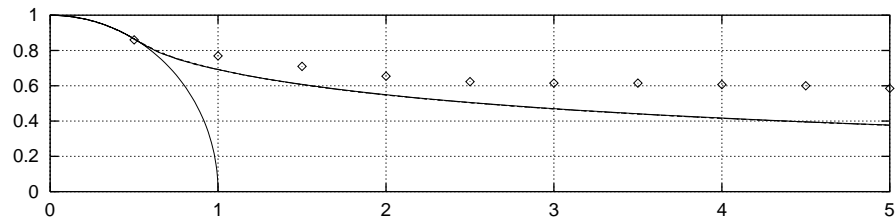
## 5. Results and Discussion

The scheme and algorithm were tested for practical consistency of the approximation by means of exhaustive numerical experiments involving different mesh resolutions. The solution depends on the adequate choice for the “actual infinities”  $\eta_\infty, \tau_\infty$  and the spacings  $h_i, g_j$ . The “optimal” parameters have been selected after extensive numerical experiments. For instance, the practical value for the relaxation parameter turned out to be  $\omega = 0.01$ . Smaller values increased intolerable the computational time while  $\omega > 0.1$  could not ensure the convergence of the global iterations. Respectively  $\eta_\infty = 10$  is the optimal value for the lateral “actual infinity”

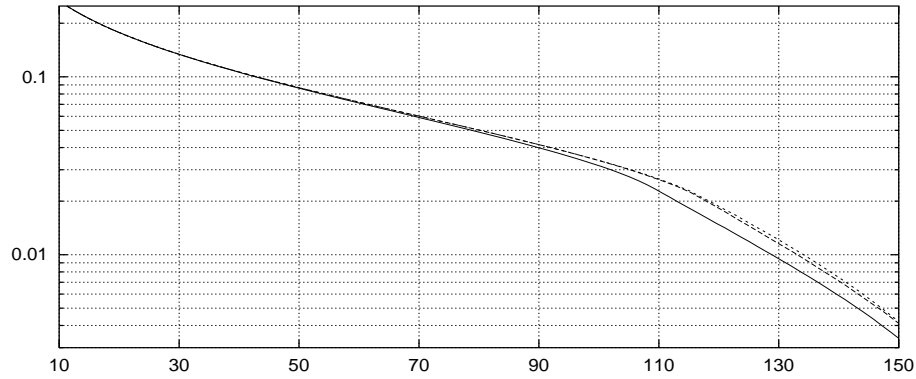
In Figs. 1-a,b is presented the obtained shape of the stagnation zone near the body and in the far wake, respectively. The symbols stand for the results taken from the charts of the paper [13]. It is seen that up to 100 calibres our calculations with different mesh parameters compare among themselves quantitatively very well. The logarithmic scale is used in Fig. 1-b in order to expand the difference between to solutions making it visible in the graph. This supports the claim that indeed a solution to the Helmholtz problem has been found numerically by means of the developed in the present work difference scheme.

The calculated here dimensionless pressure  $q$  is shown in Fig. 2. In the stagnation zone it is of order of  $10^{-4}$ , which is in very good agreement with the assumption that the unknown boundary is defined by the condition  $q = 0$ . The amplitude of the minimum of  $q$  is smaller than 3 the latter being the value for ideal flow without separation. This means that the stagnation zone influences the flow upstream.





(a) the near wake,



(b) the far wake,

Figure 1: The separation lines for relaxation parameter 0.01 and different resolutions: - - - 81x136; - - - 101x136; — 101x201;    Sowthwell and Vaisy.

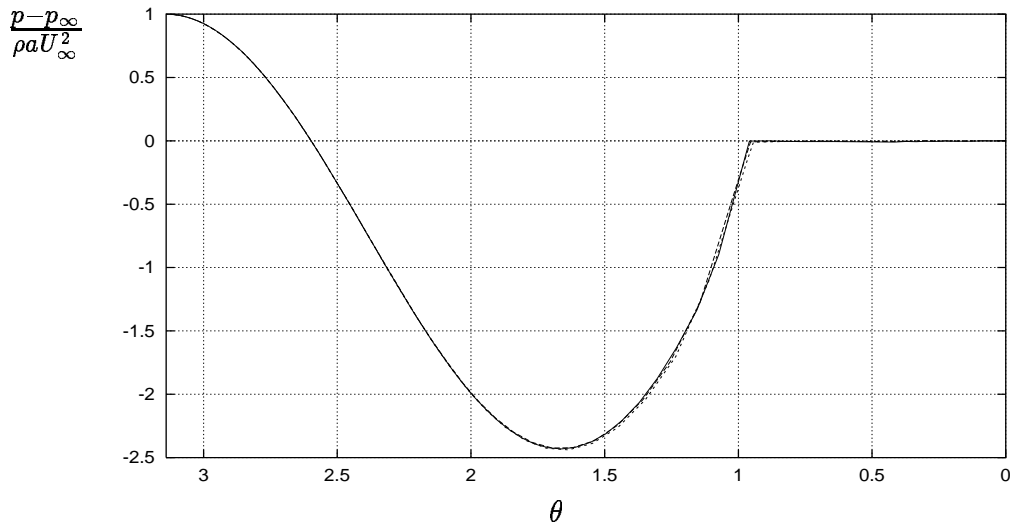


Figure 2: The pressure distribution for relaxation  $\omega = 0.01$  and different resolutions: - - - 81x136; - - - 101x136; — 101x201.

## 6. Concluding Remarks

The separated inviscid flow behind a circular cylinder is treated as a flow with free surface – the boundary of the stagnation zone (Helmholtz problem). Scaled coordinates are employed rendering the computational domain into a region with fixed boundaries and transforming the Bernoulli integral into an explicit equation for the shape function. Difference scheme using ordinate splitting is devised. Exhaustive set of numerical experiments is

run and the optimal values of scheme parameters are defined. Results are verified on grids with different resolutions. The obtained here shape of the stagnation zone is of infinitely long cusp which confirms a long forgotten numerical result of [13].

**Acknowledgment** This work was supported in part by Grant MM-602/96 of the National Science Foundation of Bulgaria.

## References

- [1] G. Birkhoff and E. H. Zarantonello. *Jets, Wakes, and Cavities*. Academic Press, New York.
- [2] S. Brodetsky. Discontinuous fluid motion past circular and elliptic cylinders. *Proc. Roy. Soc., London A*, 718:542–553, 1923.
- [3] C. I. Christov and M. D. Todorov. Numerical investigation of separated or cavitating inviscid flows. In *Proc. Int. Conf. Num. Methods and Applications, Sofia 1984*, pages 216–233, 1985.
- [4] C. I. Christov and M. D. Todorov. On the determination of the shape of stagnation zone in separated inviscid flows around blunt bodies. In *Proc. XV Jubilee Session on Ship Hydrodynamics, Varna, 1986*, Varna, 1986. BSHC. paper 10.
- [5] C. I. Christov and M. D. Todorov. An inviscid model of flow separation around blunt bodies. *Compt. Rend. Acad. Bulg. Sci.*, 7:43–46, 1987.
- [6] C. I. Christov and P. Volkov. Numerical investigation of the steady viscous flow past a resting deformable bubble. *J. Fluid Mech.*, 153:341–364, 1985.
- [7] B. Fornberg. A numerical study of steady viscous flow past a circular cylinder. *J. Fluid Mech.*, 98:819–855, 1980.
- [8] B. Fornberg. Steady viscous flow past a circular cylinder up to Reynolds number 600. *J. Comput. Phys.*, 61:297–320, 1985.
- [9] H. Helmholtz. Über discontinuirliche flüssigkeitsbewegungen. In *Monatsbericht. d. Akad. d. Wiss., Berlin*, pages 215–228, 1868.
- [10] I. Imai. Discontinuous potential flow as the limiting form of the viscous flow for vanishing viscosity. *J. Phys. Soc. Japan*, 8:399–402, 1953.
- [11] B. Kawaguti. Discontinuous flow past a circular cylinder. *J. Phys. Soc. Japan*, 8:403–406, 1953.
- [12] G. Kirchhoff. Zur theorie freier flüssigkeitsstrahlen. *J. Reine Angew. Math.*, 70:289–298, 1869.
- [13] R. V. Southwell and G. Vaisy. *Phil. Trans.*, A240:117–161, 1946.
- [14] M. D. Todorov. Christov's algorithm for Helmholtz problem: an integral-equations implementation. In *Proc. XVIII National Summer School "Application of Mathematics in Technology", Varna, 25.8.-2.9.1992*, pages 191–193, Sofia, 1993.
- [15] H. Villat. *Sur la resistance des fluides, Apercus theoriques*. Number No 38. Gauthier-Villars, Paris, 1920.
- [16] N. N. Yanenko. *Method of Fractional Steps*. Gordon and Breach, 1971.

*Institute of Meteorology and Hydrology,  
Bulgarian Academy of Sciences,  
66 Tsarigradsko Chaussee,  
Sofia 1784, Bulgaria*

*Dept. of Differential Equations,  
Institute of Mathematics and Informatics,  
Technical University of Sofia,  
Sofia 1126, Bulgaria*